Research article

Neurons, Muscles, and Venom: Identifying Drivers of Cephalopod Predation

Kim N. Kirchhoff [1,2], Melvin Williams [1], Belkes Stambouli [1,2], José Ramón Pardos-Blas [1], Amy Courtney [3], Andrew L. Sugarman [4], Daniel J. Vanselow [4], Christian Carrasco [1], Cecilia Cuddy [5], William R. Schafer[3,6], Keith C. Cheng [4], Eve Seuntjens [6], Mandë Holford [1,2,7]*

[1] Department of Chemistry, Hunter College, CUNY, NYC, NY, USA
[2] Programs in Biology, Biochemistry, and Chemistry at CUNY Graduate Center, NYC, NY, USA
[3] MRC Laboratory of Molecular Biology, Cambridge, United Kingdom
[4] Department of Pathology, Pennsylvania State University College of Medicine, Hershey, PA, USA; Institute for Computational and Data Sciences, Pennsylvania State University, University Park, PA, USA
[5] Laboratory of Molecular Biology, The Rockefeller University, NYC, NY, USA
[6] Department of Biology, KU Leuven, Leuven, Belgium
[7] Department of Invertebrate Zoology, The American Museum of Natural History, NYC, NY, USA

* Correspondence: mholford@hunter.cuny.edu

Abstract

Coleoid cephalopods (octopuses, squids, and cuttlefish) produce venoms in their posterior salivary glands. Despite venom's importance in cephalopod evolution and ecology, its regulation and secretion processes remain unresolved. Here, we performed multimodal histological profiling and live imaging to map the glandular architecture and innervation patterns across multiple coleoid species. Micro-computed tomography and tetrachrome alongside hematoxylin and eosin stains verified the proposed differentiation of gland tubular structures into (i) secretory tubules - for venom production - and (ii) striated tubules - potentially propelling venom towards the salivary duct. By tracing five neuronal markers, including nicotine acetylcholine receptors and synapsin, we observed dense neural networks intimately associated with localized muscular signals surrounding the tubules. These findings reveal a spatially distinct organization of venom production and release sites and strongly indicating that neuromuscular signals coordinate venom release into the salivary duct. Although the precise neural circuitry remains to be mapped, our results offer novel understanding of venom gland regulation in marine venomous invertebrates.

Teaser

Venom producing posterior salivary glands in octopus, squid and cuttlefish underlie neuromuscular control for focal venom release.

Introduction

Mollusks are the second-largest animal phylum, within which cephalopods (approximately 800 species) stand out for their complex cognition, camouflage, and highly developed central brain (1,2). Although these traits have attracted substantial research attention, cephalopod use of venom for predation remains understudied. Venoms are complex biochemical cocktails—often composed of small molecules, peptides, and proteins—that have convergently evolved across major animal lineages (3,4) and have demonstrated therapeutic relevance5. Despite the prevalence of venom in nature, the mechanisms underlying their biological processes such as production, regulation and release are not well understood.

Marine venomous organisms like cnidarians (*e.g.,* jellyfish) and coleoid cephalopods (octopuses, squids, cuttlefish) comprise some of the oldest venomous creatures dating back 500 million years (6) (Fig. 1a). Coleoid's specialized venom system comprises their posterior salivary gland (PSG), which can be single (in squids) or paired (in cuttlefish and octopuses), and is hypothesized to be the primary venom producing tissue (Fig. 1b). In the PSG, venom is stored in secretory granules that are released to the salivary papilla via the salivary duct, ultimately entering the buccal mass to enable immobilization of the prey (7,8) (Fig. 1b-d and Fig. S1). The question of how external stimuli trigger venom secretion remains unanswered. Prior studies suggest venom release is triggered by dual innervation of the PSG. Specifically, the superior buccal lobe innervates the basal membrane in the secretory tubules of the gland, while the fibers of the subradular ganglion regulate the smooth muscles in the gland and those associated with the salivary duct and papilla (7,9,10). However, proof of this venom release mechanism, neuron types, and the neurotransmitter systems have yet to be experimentally identified.

This study addresses the venom release knowledge gaps by conducting a comprehensive histological profiling of the potential neural and muscular organization in PSGs across all three venomous coleoid cephalopod lineages (Fig. 1b). Using *Doryteuthis pealeii* (longfin inshore squid), *Euprymna berryi* (hummingbird bobtail squid with paired PSG), *Sepia bandensis* (dwarf cuttlefish), *Sepia officinalis* (common cuttlefish) and *Octopus bimaculoides* (California two-spot octopus), we applied tissue-specific markers and *ex vivo* live staining recordings to differentiate muscular and neuronal tissue, analyze their distribution patterns, identify commonly known neuronal components and potential neuronal signaling pathways.

This work integrates structural, cellular, and neuromuscular signals to provide the first comparative neuronal characterization of coleoid venom glands. Our findings offer a holistic perspective on neuro-regulation of venom release mediated via nerves modulating smooth muscle contraction, and establishes a foundation for future studies on venom gland activation and release in one of the oldest venomous lineages.

Results

Conserved posterior salivary gland structure across coleoid lineages

To determine if there are differences in the venom secreting tissue across coleoids, we performed morphological characterization of PSGs in squid (*E. berryi*), octopus (*O. bimaculoides*), and cuttlefish (*S. bandensis*) specimens. Micro-computed tomography (micro-CT) reconstructions of the PSG in an *O. bimaculoides* hatchling indicate two differentiated tubule types distinguished by morphology and clear differences in texture

(Fig. S2). The two types present correspond to secretory and striated tubules, as previously alluded to (10,13) (Fig. 1c,d). Herein, proximal-striated tubule refers to those in proximity

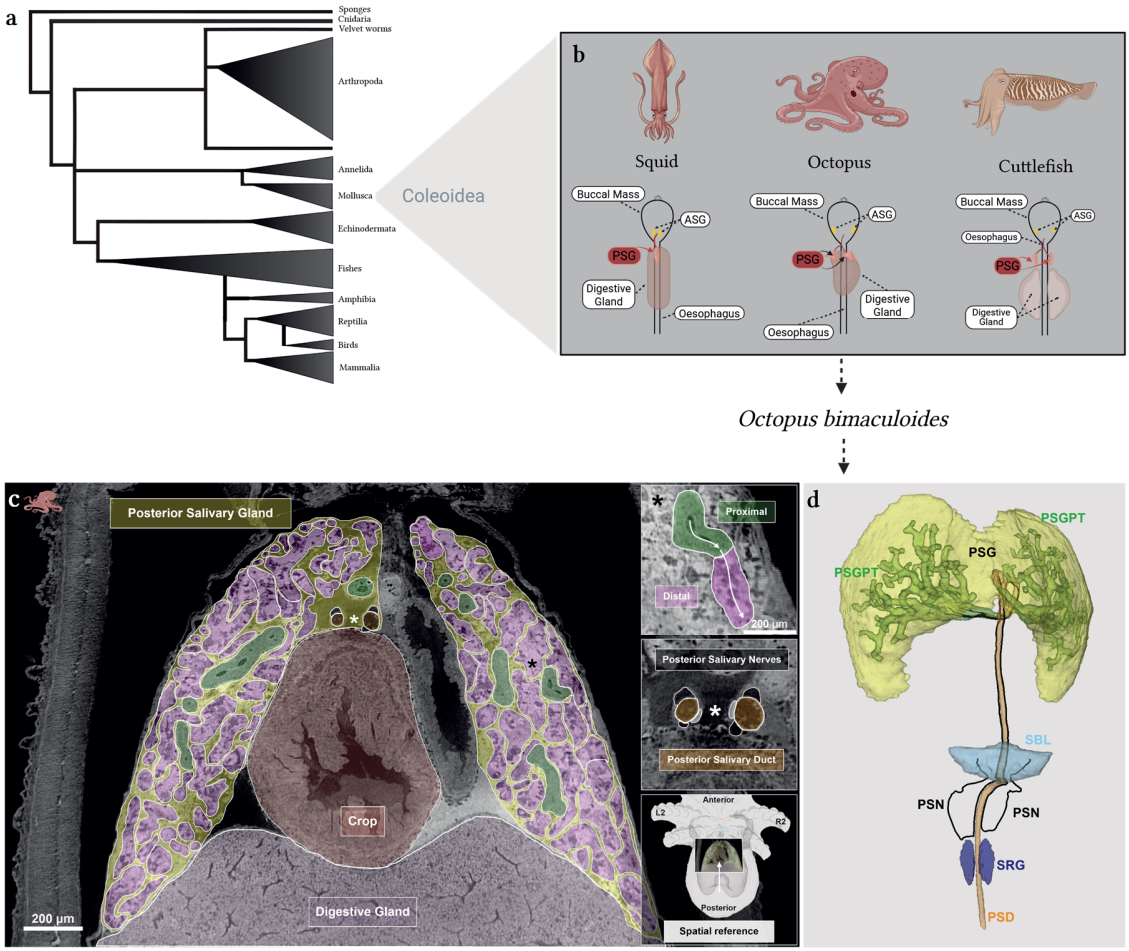

Figure 1. Cephalopods produce venom in their posterior salivary gland, which can be paired or single. a, Phylogenetic tree of venomous animal taxa highlighting the position of venomous coleoid cephalopods, *i.e.* octopuses, squids, and cuttlefish (adapted from (11)). **b,** Anatomical description of the venom system in coleoid lineages comprising the posterior salivary gland (PSG), *i.e.* venom gland (single or paired), venom duct, salivary papilla and buccal mass (dorsal view; adapted from (12) in BioRender https://BioRender.com). **c,** Micro-computed tomography (CT) 2D reconstruction of a transversal single 4 µm section of an *Octopus bimaculoides* hatchling shows the paired PSGs, proximal-striated (green) and distal-secretory (pink) tubules, posterior salivary nerves (black), posterior salivary duct (PSD) and digestive gland (purple) in corresponding color code to the following 3D model. **d,** Micro-CT based 3D reconstruction highlights the segmentation of the gland's tubular system (PSGT; green) as well as neuronal tracing from the posterior salivary nerve fibers (PSN; black) of the superior buccal lobe (SBL; light blue) to the PSG (yellow) in *O. bimaculoides* hatchling. The subradular ganglion (SRG; dark blue) and PSD positions are also shown.

to the posterior salivary duct (PSD), and the distal-secretory tubule are distal to the PSD (Fig. 1 and Fig. S2). Hematoxylin and eosin staining revealed a consistent branching architecture of numerous small tubular structures (100 - 150 µm) with heterogenous diameters and lumen sizes (Fig. 2a,b). These findings align with previous descriptions of the PSGs in *S. officinalis* (14) and *Octopus vulgaris* (15). Tetrachrome staining of PSG sections in *E. berryi* further display granules, high protein content, and distinctive tissue layers between tubules potentially involving mucopolysaccharids (Fig. 2c,d). On a cellular

level, transmission electron microscopy (TEM) images confirm an affluence of secretory granules and mitochondria in the secretory epithelial cells of *E. berryi*, *O. bimaculoides* and *S. bandensis* (Fig. 2e-g). Taken together, the general morphology of PSGs across coleoid taxa is consistent in tubular distribution and structure, with few differences on a cellular-level such as abundance of secretory granular and mitochondria, which may vary based on stage of development, venom release, position within the gland or type of tubule.

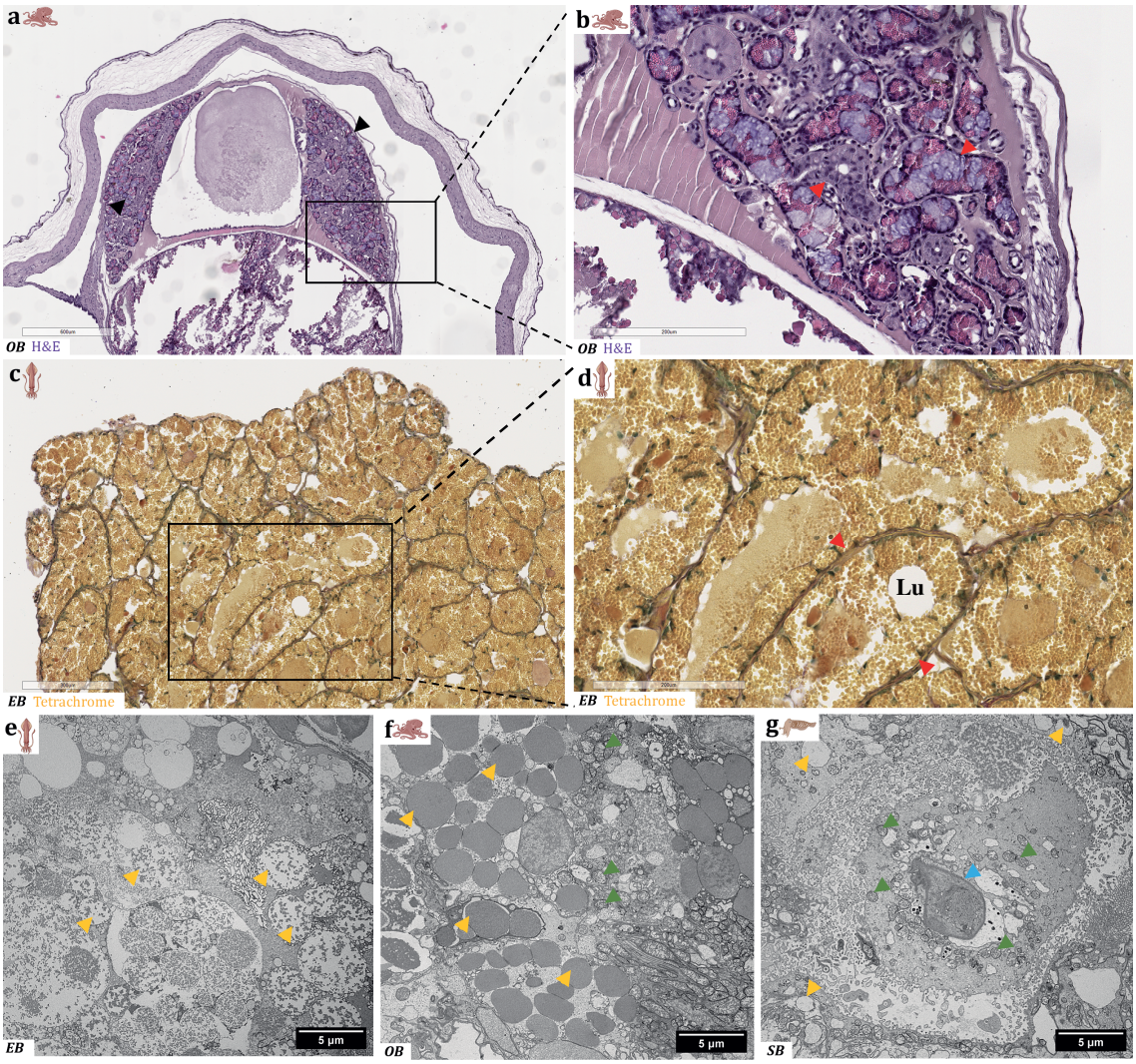

Figure 2. Histological characterization of coleoid posterior salivary glands (PSGs) reveal cross-lineage structural similarities. a,b, Hematoxylin and eosin staining of a formalin fixed, paraffin-embedded section of the PSG of adult *Octopus bimaculoides*. Arrowheads: PSG (black), tubules (red). **c,d,** Tetrachrome staining in a paraformaldehyde fixed, paraffin-embedded section of the PSG of an adult squid *Euprymna berryi*. Lu = Lumen, arrowheads: tubules (red). **e-g,** Transmission electron microscopy images from the PSG of *E. berryi* (e), *O. bimaculoides* (f), and *Sepia bandensis* (g) highlighting abundant secretory granules and mitochondria. Arrowheads: secretory granules (yellow), mitochondria (green), nucleus (blue).

Neuronal and Neuromuscular communication sites are present in PSGs

To identify potential neuronal pathways in venom release, we stained PSG tissue sections of squid (*E. berryi*, *D. pealeii*) and octopus (*O. bimaculoides*) for presynaptic vesicle-

associated phosphoproteins (synapsin), which participate in neurotransmitter release (16). Synapsin control staining in *S. bandensis* tentacles confirmed marker specificity and revealed strong central and peripheral signals consistent with known neuronal bundles and epidermal innervation (Fig. 3a). The synapsin signals recorded in the PSGs were widespread around the tubular structures, aligning with densely clustered cell nuclei and no luminal staining (Fig. 3b-e). The signal distribution is further congruent with the actin pattern observed, although synapsins are less localized and with lowest signal intensity in *O. bimaculoides* (Fig. 3c).

To characterize specific receptors, we examined the presence/absence of α-nicotinic acetylcholine receptors (nAChRs), which are abundant at neuromuscular junctions (NMJs) using the snake venom neurotoxin, α-bungarotoxin that binds with high affinity to muscle-type and low affinity to certain neuronal nAChRs (17). The specificity of this staining was confirmed in *S. officinalis* arm suckers (Fig. 3f-g), with sharp peripheral signals where NMJs are present. In the PSGs of cuttlefish (*S. officinalis*, *S. bandensis*), α-nAChR signals were recorded in the gland periphery and diffuse staining between tubular structures (Fig. 3h-l). Additionally, phalloidin staining revealed actin filaments grouped around the tubular structures in the PSG of *O. bimaculoides*, which strongly support the proposed circular smooth muscle layer around the secretory tubules in octopus PSG (10). The phalloidin signal was specific and localized around tubules, matching DAPI-stained cell body aggregation potentially highlighting high abundance of muscle fibers (Fig. 3m). These findings indicate that the machinery for neuronal synapses-activity, neuromuscular junctions, and α-nAChRs are present in the PSGs of cephalopods.

A network of neural structures and agents identified throughout the coleoid PSGs

To further characterize the type of neuronal structure and receptors present in coleoid PSGs, we investigated neuronal structural and molecular elements beyond the synaptic interface, revealing a complex network with peripheral neuronal clusters potentially acting as signal hubs. Neuronal nuclei (NeuN)-positive cell bodies, abundant Nissl substance, and choline acetyltransferase (ChAT) expression are indicators for neuronal components and potential cholinergic signaling typical of neuronal tissue and neuromuscular junctions (NMJs). In PSG tissue sections of *S. bandensis,* NeuN staining—marking mature neuron nuclei and perinuclear cytoplasm—is prominent as small, round clusters near the peripheral tubular openings and extends between the tubular structures until the center of the gland, with luminal areas devoid of staining (Fig. S3a). Similarly, in *D. pealeii* PSG, darkly stained round structures at the gland periphery suggest Nissl bodies – large aggregates of endoplasmic reticulum and ribosomes – are present in neuronal somas whose high rRNA content was targeted (Fig. S3b). High gene expression in glandular tissue, however, necessitates additional markers to distinguish neuronal from secretory cell-related nucleic acids.

Characterization of squid *D. pealeii* PSG with ChAT, choline acetyltransferase, essential for acetylcholine production in cholinergic neurons and NMJs, exhibit potentially higher expression at the periphery of the PSG, and less intensity throughout the gland (Fig. 3 n-o). The ChAT experiments were conducted using *in situ* hybridized probes originally designed from *Octopus bocki* ChAT sequences, while newly designed probes for *D. pealeii* cephalotoxin-2 (ctx-2) sequences (18), were used to visualize this highly expressed venom transcript in the gland sections along with cell nuclei (DAPI). While ChAT expression supports the presence of acetylcholine-producing motor neurons, single-channel recordings

showed limited differentiation between ctx-2 and ChAT patterns, maybe indicating proximity in the expression of venom ctx-2 and cholinergic neurons (Fig. S3c-d). These results are the first experimental proof of a network of neuronal agents that may act in concert to facilitate venom release from PSGs.

Live staining of squid PSG explant suggests calcium signaling activation

To monitor potential transmission of neuronal signaling, we examined if calcium signaling could be recorded in *ex vivo* cephalopod venom glands. Specifically, we incubated explanted PSGs from *E. berryi*, with a cell-permeable fluorogenic calcium indicator. Calcium plays a versatile role in the nervous system, but also in muscular tissue, acting as a second messenger and facilitating presynaptic exocytosis, postsynaptic signaling, and action potential development (19,20). Using this technique we observed spontaneous calcium activity, particularly in areas resembling circular nuclear regions near the edge of the PSG (Fig. 3p; see Movie S1). We also observed waves of calcium activity within thin processes travelling between these regions. Further analyses are required to determine if this activity is neural or muscular, and what neurotransmitters or neuromodulators would cause direct activation of these cells. However, while the *in vivo* analysis presented here is a pilot study, it demonstrates the suitability for in-depth assessment of signaling pathway activation and modulation in a real-time live staining setting for cephalopod venom gland explants.

Discussion

Complex neuromuscular embedding potentially regulating venom release in cephalopods

Whether through pioneering work on the discovery of the squid giant axon by John Z. Young (21), or Alan Hodgkin and Andrew Huxley's (22) use of the squid giant axon to characterize the mechanism of action potentials, the Cephalopoda nervous system has been used to advance groundbreaking knowledge. However, the cephalopod venom system has been mostly overlooked. Here, we begin to unravel the mechanics on neuronal control of venom release for prey capture in cephalopods. Our results indicate that octopuses, squids, and cuttlefish share highly conserved microanatomical components of their posterior salivary gland, *i.e.* venom gland. Specifically, PSGs are characterized by branching glandular tubules that are infiltrated by muscle fibers and connective tissue containing blood vessels and nerve fibers, as described in *Octopus* spp. (13,14). These tubules have varying dimensions and luminal area size that are potentially dependent on tissue section orientation and apical or basal localization with respect to the transition to the posterior salivary duct. A major finding is the visualization of striated and secretory differentiated patterns in PSG tubules. This differentiation indicates distinct parts of the tubules may be used to "push" venom through the gland and to secrete venom into the posterior salivary duct, underscoring a potential muscle-driven mechanism for venom release.

Current proposals for venom release include, apocrine secretion, which involves budding of cellular cytoplasm, and is typical for mammalian salivary glands (23). However holocrine secretion, which involves bursting of cells, is proposed for molluscan cone snails (24). While the venom secretion mechanism of any venomous snail or cephalopod remains to be elucidated, the neural, neuromuscular and muscular signals presented here support the hypothesis of neuromuscular control of the PSG in cephalopods, with muscular fibers around the secretory tubules and a marked innervation pattern across the gland. The localized and high-affinity signals of nAChR, and the abundant synapsin observations,

suggest a dual innervation mechanism for neuronal connectivity and venom release stimulation pathway as proposed by Young (5) and House (8). The neuronal and neuromuscular recordings in this study provide the first coherent insights into the interplay between neuronal and glandular systems in cephalopods, a significant first step in delineating the venom release neural circuit. Similar observations of neural innervation in spiders (25), scorpions (26), snakes (27) and the giant centipede (28) venom glands have been reported and point to a widespread phenomenon of neuronal control of venom release throughout vertebrates and invertebrates. This further supports the importance of non-model systems in furthering scientific discovery.

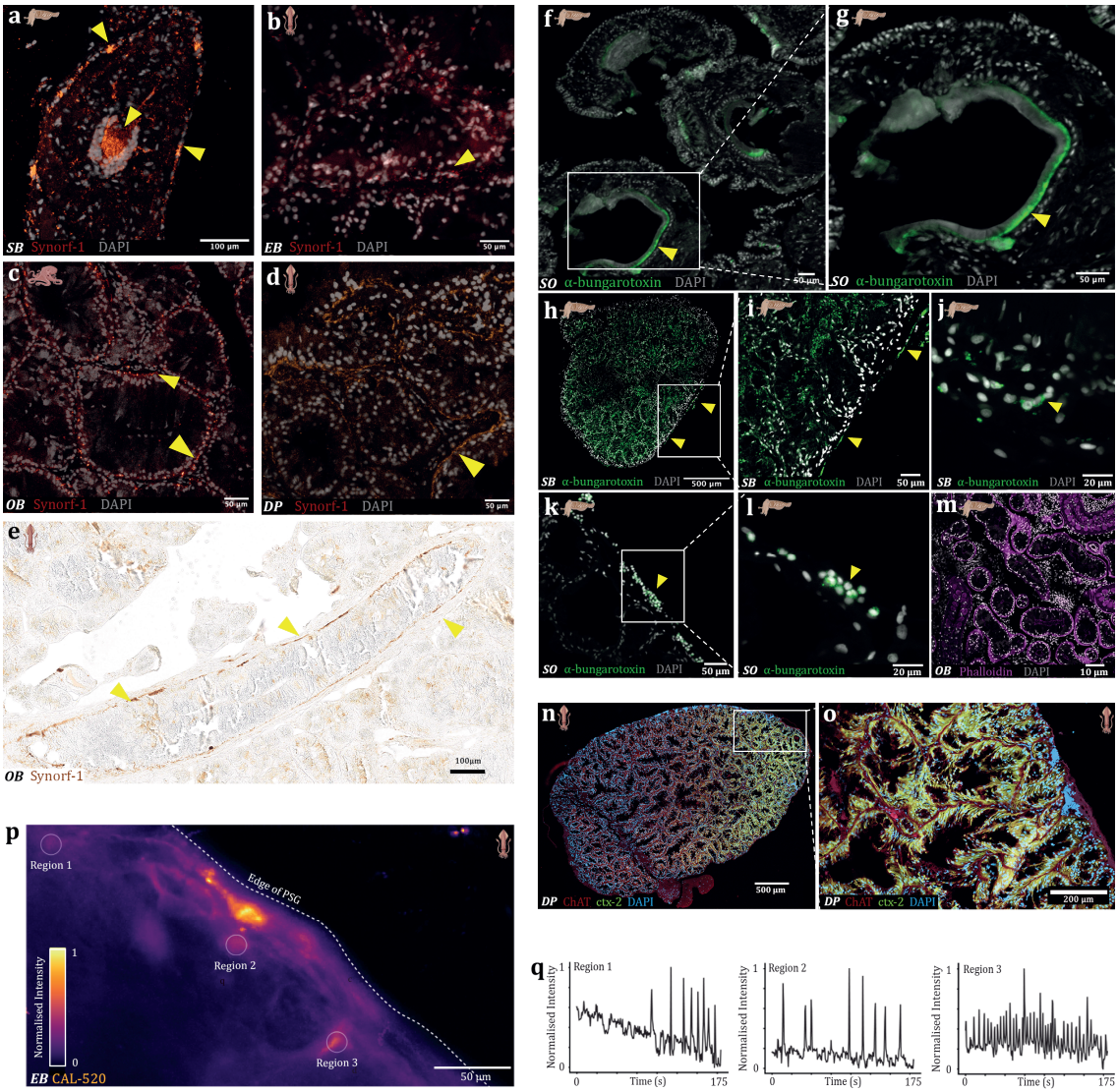

Figure 3. A network of neural agents is present in the posterior salivary glands (PSGs) of coleoid cephalopods. a-e, Synapses were highlighted by staining phosphoproteins known to abundantly appear in presynaptic cytoplasma (Synapsin; Synorf1 marker) along with cell nuclei staining (DAPI: grey) in **a,** the tentacle section of adult *Sepia bandensis (SB)*, and the PSG sections of adult **b,** *Euprymna berryi (EB)*, **c,** *Octopus bimaculoides (OB)*, and **d, e,** *Doryteuthis pealeii (DP)*. **f-l,** Neuromuscular junctions were highlighted by labeling the alpha subunit of the muscle-type nictoinic acetylcholine receptor with α-bungarotoxin (α-nAChR: green) in the context of cell density by nuclei staining (DAPI: grey) in **f, g,** paraffin

sections of the arm suckers and **k, l,** the PSG of adult *Sepia officinalis (SO)*, and **h-j,** *S. bandensis* under different magnification. **m,** Muscular fiber distribution throughout a paraffin section of the PSG in *O. bimaculoides* was visualized by staining actin filaments (Phalloidin: purple) along with cell nuclei (DAPI: grey) for highlighting cell density distribution. **n, o,** RNA-Hybridization chain reaction targeting choline acetyltransferase (ChAT: red) and cephalotoxin-2 (ctx-2), the highly expressed venom protein in cephalopods (green) in adult *D. pealeii* PSG. Cell nuclei are further stained with DAPI and all three channels are integrated in these images. **p,** Maximum intensity projection recorded in *ex vivo* PSGs of adult *E. berryi* during calcium imaging. **q,** Mean normalized intensity over time of regions 1-3 highlighted in p. Prominent signals highlighted with yellow arrowheads. The original calcium imaging recording in the ex vivo PSG can be found in the supplementary material, i.e. Movie S1.

Materials and Methods

Animals and Tissue processing

Animal specimens were obtained from the Marine Biological Laboratory, Woods Hole (MA, USA). Euthanasia was performed by gradually increasing ethanol concentration from 0 to 30% in natural sea water over 30 min. For tissue section staining, the posterior salivary glands from adult *Doryteuthis pealeii*, *Euprymna berryi*, *Sepia bandensis*, *Sepia officinalis*, and *Octopus bimaculoides* were dissected and processed as described below. Briefly, after dissection, the gland samples were fixed overnight (at least 16 h) in 4% paraformaldehyde in artificial salt water at 4°C. Fixed samples were washed with DEPC-treated PBS and gradually dehydrated through a progressive series of ethanol, of 10% increase per 20-min steps, up to 100%. To prepare the tissues for embedding, samples were cleared with two changes of histosol (30 min each), followed by incubation in two 1:1 histosol:paraffin solution changes (30 min each) and subsequent incubation in pure paraffin overnight at 60°C. The samples underwent four to five changes in 100% paraffin, each lasting 1 h, before being transferred into sectioning molds for solidification. Paraffin blocks were sectioned at 8-10 µm thickness using a microtome. For RNA-hybridization experiments, all water and phosphate buffered saline (PBS) solutions were treated with diethylpyrocarbonate (DEPC) overnight and autoclaved before use to eliminate RNase contamination.

(Immuno)histochemistry

a. **Hematoxylin and Eosin staining.** For staining, sections were deparaffinized in xylene (2 × 5 min), rehydrated through a descending ethanol series (100%, 95%, 70%; 2 min each), and rinsed in distilled water. Slides were stained in Harris hematoxylin for 5–7 min, rinsed in running tap water for 5 min to stain the nuclei, and briefly dipped in 0.3% acidified alcohol to remove excess of dye. After another rinse with tap water, slides are being dipped into lithium carbonate for 1 min to increase staining intensity of Hematoxylin. Following another rinse in distilled water, slides were counterstained with eosin Y solution (0.5–1%) for 30 s to 2 min. After staining, sections were sequentially dehydrated through an ascending ethanol series (30%, 95%, 100%; 1 min each), cleared in xylene for 1 min, and mounted using DPX mounting medium.

b. **Tetrachrome staining.** Tetrachrome staining procedure was performed according to the protocol established by Costa and Costa (29). Briefly, tissue sections were sequentially introduced into: Alcian Blue (30 min), Milli-Q wash (2 x 30 s), 0.5% Periodic acid (5 min; Chem Impex), Milli-Q wash (at least 5 immersions), Schiff's Reagent (15 min; Sigma Aldrich), Milli-Q wash (2 x 30 s), Weigert's Iron Hematoxylin (2 min; Sigma Aldrich), running tap water (1 min), aqueous Picric acid (5 min), Milli-Q wash (at least 5 immersions). All dyes were applied in the dark and at room temperature, with the exception

of Picric Acid solution, which was preheated to 60°C before use to enhance staining. Alcian Blue (AB) was prepared with 1% m/v AB 8GX in 3% v/v acetic acid (the solution was filtered after preparation). The Weigert's Iron hematoxylin solution was prepared using a 1:1 ratio of Solution A and Solution B, as directed by Sigma. Subsequent to staining procedure, slides were dehydrated with a progressive series of ethanol, cleared with xylene and mounted in DPX resin.

c. **Filamentous Actin**. For phalloidin staining, paraffin tissue section of the PSG was incubated for 2 h at RT in the dark. Cells were counter-stained with 4',6-diamidino-2-phenylindole, dilactate (DAPI) for 10 min at RT. After each step, the cells were washed three times with PBS and mounted with coverslips (1.5 mm) and hard set mounting medium. Fluorescence was recorded at 493/517 nm.

d. **Synapsin**. Herein, we used an anti-SYNORF1 antibody (Cat.-No. 3C11, Developmental Studies Hybridoma Bank) that recognizes synapsin-1. This antibody is derived from the peptide sequence LFGGMEVCGL, located within the conserved C domain of synapsins. Its specificity has been validated across multiple species, including cephalopods. The secondary antibody was a goat anti-mouse IgG purchased from ThermoFisher (DyLightTM 650). The experimental method was adapted from Rees *et al.* (30), with modifications to suit the objectives of this study.

   The slides were rehydrated following a stepwise protocol of 2x histosol (5 min each), 2x 100% EtOH (5 min each), 75% EtOH/PBS (5 min), 50% EtOH/PBS (5 min), 25% EtOH/PBS (5 min), 2x washes in distillated water (2 min) and 3x washes in PBS supplemented with 0.1% Triton-X (5 min each). After preheating the tubes, the slides containing the PSG tissue sections were incubated in a 60°C distilled water bath for 5 min. The warmed slides were then transferred to pre-warmed antigen retrieval solution (10 mM sodium citrate, pH 6.0) and incubated at 95°C for 25 min. Subsequently, the slide container was cooled in a -20°C freezer for no more than 10 min, ensuring the slides did not freeze. The slides were then transferred to a glass Coplin jar and rinsed twice for 5 min each in PBS containing 0.1% Triton-X.

   Next, the slides were placed in a humidified chamber, and 2 ml of blocking solution (10% sheep or goat serum in PBS with 0.1% Triton) was added to each slide, followed by incubation for 1 h at room temperature. For the primary anti-body application, slides were treated with the Synorf antibody diluted in blocking solution (9.75 µg/ml, 150-200 µl per slide). Each slide was covered with parafilm and incubated overnight at 4°C in a humidified chamber.

   The following day, the slides were rinsed three times for 10 min each in PBS with 0.1% Triton, and secondary antibodies were prepared. The secondary antibody was diluted in blocking solution (3.3 mg/ml, 150-200 µl per slide), shortly centrifuged and applied to the slides, which were then covered with parafilm and incubated at room temperature in the dark for 4 h. Following this, the slides were rinsed three times for 10 min in PBS with 0.1% Triton-X, followed by three additional washes of 30-60 min each to ensure thorough removal of the secondary antibody. To ensure the experiment was working and detecting synapsin, we used brain sections as a positive control. For the negative control, additional PSG gland tissue sections from the same specimens were processed without applying the primary antibody to verify the specificity of the staining. Finally, the slides were mounted in Fluoromount-G (with or without DAPI), and glass coverslips (1.5 mm thickness) were applied. The slides were stored at 5°C and left to dry for approximately 24 h before imaging.

e. **Visualization of nAChRs at Neuromuscular Junctions:** In this study, we used α-bungarotoxin conjugates (Cat. No. B35450, ThermoFisher) to label nAChRs and visualize neuromuscular junctions in the PSG of *S. officinalis*, *S. bandensis*, and *O. bimaculoides*. α-Bungarotoxin, a peptide derived from snake venom, binds irreversibly and with high specificity to the subunit alpha of the nAChRs in muscular tissue, but has also been shown to bind with lower affinity to nAChRs in the vertebrate brain (31), making it a valuable tool for their visualization *in situ*.
The rehydration, antigen retrieval, and blocking stages followed the same protocols as of the synapsin. A concentration of 1 µg/ml α-bungarotoxin staining solution in PBS was prepared, and approximately 150-200 µL were applied per slide. Arm tissue sections were used as a positive control to confirm the detection of nAChRs, while PSG tissue sections processed without α-bungarotoxin served as negative controls to assess staining specificity. The sections were covered with parafilm and incubated at room temperature in the dark for 4 h. After incubation, the sections were rinsed three times in PBS, mounted in Fluoromount-G, and covered with a coverslip.

f. **NeuN**. Here, we used a Chromagenic DAB staining to detect the presence of neuronal nuclei with a NeuN antibody (ABN91; Merck Millipore). Stock solutions for 0.3% Triton-X/PBS (X100; Sigma Aldrich) and 0.3% Tween20/PBS (P7949; Sigma Aldrich) were made one day prior to the start of the experiment. Calculations for 3% hydrogen peroxide (H325-100; ThermoFisher), blocking solution, NeuN primary antibody solution, and secondary antibody solution were conducted the day before. The next two days follow a standard immunohistochemical procedure:
On the first day of the experiment, the slide underwent a series of rinses to deparaffinize and rehydrate with Xylene, Ethanol, and Milli-Q Water. During these rinses, 1X PBS (P3813; Sigma Aldrich) and the antigen retrieval, which was diluted with 1X Citrate Retrieval Buffer (C9999; Sigma Aldrich), were prepared and placed inside a steamer (B0BSHJ5LQ5; Elite Gourmet) for 45 min alongside an additional container of Milli-Q water. Temperature probes were used to monitor the temperature to ensure it reached 90˚C (roughly 45 min before rehydration ended). The slide rack was placed in slide well with Milli-Q water inside steamer for 10 s before transferring to slide well with antigen retrieval for 10-15 min. During this time, a humidity chamber (Stain Tray Slide Staining System, Thermo Fisher) and 3% Hydrogen Peroxide were prepared. The slides were then removed from the antigen retrieval and cooled for 20 min before being placed in a slide well with 1X PBS for 5 min. The slide was then placed inside the humidity chamber and 3% Hydrogen peroxide was added for 10 min to remove the endogenous peroxide on the tissue. Once the slide was placed in a fresh slide well with 1X PBS for 5 min, the blocking Solution was prepared. After, the slide was moved to the humidity chamber and the blocking solution was placed on the slide. While the slide was incubating at room temperature for 1 h, the NeuN primary antibody (1:100 dilution) was prepared. After the incubation, the slide was moved to the humidity chamber and the NeuN primary antibody was added before being cover slipped and left inside the humidity chamber overnight at 4˚C. On the second day, the secondary antibody (1:500 dilution) was prepared while the slide underwent 5 separate rinses with 1X PBS for 5 min each to wash off the primary solution. The secondary antibody was then placed on the slide and incubation was for 1 h before the slide was washed three times with 1X PBS for 5 min each. Then, 2-3 drops of Streptavidin (SA-5704; Vector Laboratories) were placed on the slide inside the humidity chamber for 30 min while Coplin jars were prepped with 1X PBS. As the slide was washed again in a similar sequence of

1X PBS rinses, the DAB solution (ab64238; Abcam) (40 µl chromagen to 40-45 drops of DAB substrate) was prepared. For the slide, it was placed under a microscope as the DAB solution was placed on top and sat for 1-2 min to allow for development and appearance of neuronal nuclei to appear (brown-orange color). Once complete, the slide was rinsed several times with 1X PBS before being placed in an additional slide well with 1X PBs before beginning rehydration. The slide then underwent a series of rinses with xylene and ethanol to rehydrate the slide. After, the slide was then prepared with CytoSeal XYL (18009; Electron Microscopy Sciences) and cover slipped overnight. The slide was then scanned on a digital pathology scanner (NanoZoomer-SQ Digital slide scanner, Hamamatsu Photonics K.K., Shizuoka, Japan) to observe the results.

g. **Nissl bodies**. Squid posterior salivary gland sections were used to perform a Cresyl Violet Stain (ab246817; Abcam). The slide first underwent a series of rinses that were 5 min each to deparaffinize and rehydrate the slide using xylene and ethanol. Before proceeding with the Cresyl Violet Stain, the slide sat in a slide well with Milli-Q water for 5 min. After, the slide incubated in a coplin jar with 1% Creyl Violet Stain solution for 20 min to ensure adequate time for the stain to develop on the tissue. After, the slide was washed in an additional coplin jar with Miili-Q water for 3 min to rinse off the excess Cresyl Violet and observe the stain before proceeding with the next rinses. After determining how dark the stain appeared on the tissue, the slide was incubated in 70% ethanol for 1 min and then 95% ethanol for 1 min as well to slightly rinse off excess stain but not entirely remove the stain. The slide was then incubated in xylene for 5 min before being cover slipped with CytoSeal XYL overnight. The slide was imaged the next day on a digital pathology scanner.

h. **Choline Acetyltransferase and Cephalotoxin-2:** The method was initially developed by Choi *et al.* (32) with modifications according to Criswell and Gillis (33). Hybridization Chain Reaction (HCR) reagents where obtained from Molecular Instruments Inc. (LA, USA), where probes for the venom protein cytotoxin-1 for *D. pealeii* were further specifically designed. The probes for choline acetyltransferase were previously designed for *Octopus bocki* (18), and here tested on *D. pealeii* PSG sections. Sequences upon which the hybridized probes were designed can be found in the supplemental Table S1.
Slides were deparaffinized twice in histosol for 5 min. Slides were then rehydrated in a series of decreasing ethanol solutions: 100% ethanol for 5 min ×2, then 2 min each in 90%, 70%, and 50% ethanol/DEPC-PBS, DEPC water, and DEPC-PBS with 0.1% Tween20. Subsequently, slides were treated with 10 µg/ml proteinase K (25530049; Thermo Fisher) in DEPC PBS at 37°C for 10 min and rinsed in DEPC water at room temperature for 2 min. Slides were moved to a humidified chamber for and pre-hybridized by adding 2 ml of pre-warmed hybridization buffer per slide. Slides were incubated in the humidified chamber at 37°C for 30 min. During this pre-hybridization step, probe sets were diluted in pre-warmed hybridization buffer, with 0.8 µl of each 1 µM probe stock added per 100 µl of hybridization buffer, preparing 300 µl of hybridization buffer per slide, and the mixture was returned to 37°C. After the 30 min pre-hybridization, the humidified chamber was removed from the 37°C incubator and 250 µl of hybridization buffer with the probe was added to each slide. A parafilm coverslip was set over each slide and they were incubated in a humidified chamber at 37°C overnight. On the second day, parafilm was carefully removed, and slides were briefly washed twice with around 1 ml of pre-warmed HCR wash buffer. Then, slides were washed at 37°C with the pre-warmed solutions as follows: 75% wash buffer for 15 min, 50% wash buffer for 15 min, 25% wash buffer for 15 min, and 5x SSCT for 15 min. Slides were then washed in 5x SSCT at room temperature for 5 min. To prepare the hairpins,

8 µl of each hairpin solution (H1 and H2) were heated separately in microcentrifuge tubes to 95°C for 90 s and then cooled in the dark at room temperature for 30 min. Hairpin solution were proportionally prepared for a final volume of 200 µl of amplification buffer with hairpins per slide. Slides were moved to a humidified chamber and pre-amplified by applying 2.5 ml of room temperature amplification buffer to each slide. Slides were incubated in the humidified chamber for 30 min at room temperature. Hairpins and amplification buffer were then mixed and briefly vortexed, the pre-amplification buffer was drained off, and 200 µl of this mixture was added to each slide. A parafilm coverslip was added, and the slides were incubated in a humidified chamber overnight in the dark at room temperature. On the third day, slides were washed in the dark as follows: 5x SSCT for 5 min, twice with 5x SSCT for 15 min, and 5x SSCT for 5 min. Glass coverslips (1.5 mm thickness) were applied with Fluoromount-G with DAPI. Slides were stored in the dark and allowed to dry overnight before being stored at 4°C in the fridge.

i. **Live calcium signaling.** PSG was dissected from *E. berryi* specimen immediately after euthanasia, and placed in a petri dish with cell culture medium, herein called octomedia. Octomedia was prepared as follows; (in mM) NaCl: 214.04, $MgSO_4x7H_2O$: 26.17, KCl: 4.61, NaHCO3: 2.29, $MgCl_2x6H_2O$: 28.04, D-glucose: 38.08 $CaCl_2x2H_2O$: 10.12, and 500 ml L-15, Leibowitz, with L-glutamine (Sigma, MFCD00217482). Octomedia was adjusted to pH 7.6-7.7 with KOH, and filtered using the corning system (431098), stored at 4°C and used within one week. The calcium indicator CAL-520 (Abcam, UK) was prepared at 5 mM in DMSO, and stored at -20°C. CAL-520 improves signal-to-noise ratios compared to standard calcium imaging, allowing live fluorescence recordings of calcium migration within the PSG (34). PSGs were incubated in CAL-520 (5 µM in Octomedia) for 15 min. Imaging was performed with an upright epifluorescent microscope equipped with a 490/525 nm excitation/emission filter set and operated at 2fps. Calcium imaging videos were processed as follows; image registration was performed within suite2p using the non-rigid registration approach (35), spontaneously active regions were manually defined, normalised using a min/max approach and plotted using a custom python script. The maximum intensity projection image shown in Fig. 3 was prepared for publication using ImageJ (36,37).

Microscopy and Image Processing

Several different imaging techniques were employed to visualize the models, histological details, and staining results.

a. **Electron Transmission Microscopy**: Samples were washed with PBS, then fixed with a modified Karnovsky's fix of 2.5% glutaraldehyde, 4% paraformaldehye and 0.02% picric acid in 0.1M sodium caocdylate buffer at pH 7.2 (38). Following a secondary fixation in 1% osmium tetroxide, 1.5% potassium ferricyanide, samples were dehydrated through a graded ethanol series, and embedded in an epon analog resin. Ultrathin sections were cut using a Diatome diamond knife (Diatome, USA, Hatfield, PA) on a Leica EMEC7 ultramicrotome (Leica, Vienna, Austria). Sections were collected on copper grids and contrasted with lead citrate (39) and viewed on a JEM transmission 1400 electron microscope (JEOL, USA, Inc., Peabody, MA) operated at 100 kV. Images were recorded with a Veleta 2K x2K digital camera using RADIUS software (EMSIS, Germany).

b. **Micro-Computer Tomography**: an *O. bimaculoides* hatchling was obtained from the Marine Biological Laboratory and anesthetized in sea water with several percent ethanol

and placed in a fixative of 4% paraformaldehyde in sea water for several days. The hatchling was immersed for a week in phosphotungstic acid and eosin solution, rinsed several times with distilled water, and then chemically dehydrated with acidified 2-2-di-methoxypropane (DMP) overnight. It was then immersed in hexamethyl di-silazane (HDMS) and air dried overnight in a hood. The intact animal was glued to an aluminum SEM stub mounted with plasticine onto a ThorLabs half inch diameter optical post screwed into a 1x1" kinematic base for imaging.

Parallel beam synchrotron X-ray imaging was performed at sector 2 bending magnet beamline (2BM) of the Advanced Photon Source (APS) of Argonne National Laboratory. The beam energy was monochromatic and set to 25.5 keV and a sample to scintillator distance of 70 mm was used. Two sets of 9001 X-ray projections were collected over 360 degrees of sample rotation to reconstruct the hatchling. 28% overlap between tomograms was chosen to minimize stitching artifact. Each projection was captured using a custom wide-field detector and camera with a 10mm field-of-view (FOV) and 0.7 μm^4 voxel size. The 3D reconstructions were calculated using the gridrec algorithm from TomoPy and stitched with manual alignment in ImageJ (36,37). The Bronnikov Aided Correction was used for phase retrieval with alpha and beta parameters equal to 2.0 (40,41).

c. **Confocal microscopy**: the phalloidin, synorf-1 (Fig. 3a-d), NMJ, ChAT, and *ex vivo* imaging was performed using a Zeiss LSM 880 confocal microscope equipped with 10x, 25x, 40x, and 63x objectives. Image processing was performed with the Zeiss Zen 3.10 blue version software.

d. **Light microscopy:** synorf-1 (Fig. 3e), NeuN and Nissl bodies stained tissue sections were captured with either a Zeiss Axioscope 5 at a resolution of 1024 × 1024 pixels or a Nikon Eclipse E400 microscope. Images were processed with Image J Fiji software and, the latter, with Omax ToupView software v.4.11 (Caltech, USA).

e. **Digital Slide scan:** tetrachrome and H&E tissue slides were scanned at 40× using an Aperio AT2 slide scanner (Leica Biosystems, Nussloch, Germany) and images were saved in TIFF format. Image processing was made with the manufacturer ImageScope software.

References

1. Mather, J.A.; Kuba, M.J. *Can J. Zool.* **2013** *91*, 431-449.
2. Allock, A.L., Lindgren, A., Strugnell, J.M. *J. Nat. His.* **2015** *49*, 1373-1421.
3. Holford, M. et al. *Science* **2018** *361*, 842-844.
4. Schendel, V.; Rash, L.D.; Jenner, R.A; Undheim, E.A. *Toxins* **2019** *11*, 666.
5. King, G.F. (Ed.). *Royal Society of Chemistry* **2015**.
6. Albertin, C.B.; Katz, P.S. *Curr. Biol.* **2023** *33*, R1087-R1091.
7. Young, J.Z. *Philos. Trans. R. Soc. Lond. B. Biol. Sci.* **1965** *249*, 27-44.
8. Gibbs, P.J.; Greenaway, P. *Toxicon* **1978** *16*, 59-70.
9. Young, J.Z. J. *Exp. Biol.* **1965** *43*, 581-593.
10. House, C.R. *Biol. Rev.* **1980** *55*, 417-473.
11. Gorson, J.; Holford, M. *Int. Comp. Biol.* **2016** *56*, 962-972.
12. Hanlon, R.; Vecchione, M.; Allcock, L. University of Chicago Press, USA, **2018**.
13. Anadón, R. Handbook of pathogens and diseases in cephalopods, Gestal, C., et al. (eds.); Springer, Cham, UK, **2019**; pp. 39-85.
14. Gonçalves, C.; et al. *Front. Mar. Sci.* **2024** *11*, 1362824.
15. Fernández-Gago, R.; Molist, P.; Rocha, F. *Acta Zool.* **2019** *100*, 320-335.

16. Klagges, B.R.; et al. *J. Neurosci.* **1996** *16*, 3154-3165.
17. Sine, S.M., Strikwerda, J.R., Mazzaferro, S. *Neuropharma.* **2019** *160*, 107660.
18. Winters-Bostwick, G.C.; et al. *Curr. Biol.* **2024** *34*, 4756-4766.
19. Grienberger, C.; Konnerth, A. *Neuron* **2012** *73*, 862-885.
20. Berridge, M.J.; Lipp, P.; Bootman, M.D. *Nat. Rev. Mol. Cell Biol.* **2000** *1*, 11-21.
21. Young, J.Z., *J. Exp. Biol*. **1938** *15*, 170-185.
22. Hodgkin, A.L., Huxley, A.F. *Nature* **1939** *144*, 710–711.
23. Farkaš, R. *Biochim. Biophys Acta* **2015** *1850*, 1740-1750.
24. Vonk, F.J.; et al. *PlosOne* **2021** *16*, e0258712.
25. Järlfors, U.; Smith, D.S.; Russell, F.E. *Toxicon* **1969** *7*, 263–264.
26. Mazurkiewicz, J.E.; Bertke, E.M. *J. Morphol.* **1972** *137*, 365–383.
27. Kerchove, C.M.; et al. *J. Exp. Biol.* **2004** *207*, 411–416
28. Schendel, V.; et al. *Nat. Ecol. Evol.* **2025** *9*, 73–86.
29. Costa, P.M., Costa, M.H. *J. Inv. Pat.* **2012** *110*, 411-414.
30. Rees, J.M. et al. *Development* **2024** *151*, dev202821.
31. Castro, N.G.; Albuquerque, E.X. *Biophysical journal* **1995** *68*: 516-524.
32. Choi, H.M. et al. *Develop.* **2018** *145*, dev165753.
33. Criswell, K.E., Gillis, J.A. *Elife* **2020** *9*, e51696.
34. Tada, M.; et al. *Europ. J. Neurosci.* **2014** *39*, 1720-1728.
35. Pachitariu, M. et al. *BioRxiv* **2016** 061507
36. Gürsoy, D. et al. *J. Synchrotron Radiat.* **2014** *21*, 1188–1193.
37. Schindelin, J. et al. *Nat. Methods* **2012** *9*: 676–682.
38. Ito, S. *J. Cell Biol.* **1968** *39*, 168A-169A.
39. Venable, J.H., Coggeshall, R. *J. Cell Biol.* **1965** *25*, 407.
40. Witte, Y.D. et al. *J. Opt. Soc. Am. A* **2009** *26*: 890–894.
41. Lohse, L.M. et al. *J. Synchrotron Radiat*. **2020** *27*: 852–859.

Acknowledgments

The authors want to express their gratitude to the Marine Biological Laboratory's Cephalopod Breeding, which resolved the husbandry of the specific species of squids (*E. berryi* and *D. pealeii*) cuttlefish (*S. bandensis* and *S. officinalis*) and octopus (*O. bimaculoides*) used in this study and thus, represents a technological springboard for the detailed study of venom biology ex situ. M.H. also acknowledges MBL Whitman Fellow Kirsten Sadler Edepli for contributions to phalloidin staining. The authors would also like to thank Roger Hanlon for contributing the *O. bimaculoides* hatchling for the micro-computed tomography and Jean Cooper for assistance with the digital scanning of presented tissue sections. The authors further acknowledge the Electron Microscopy & Histology services of the Weill Cornell Medicine Microscopy and Image Analysis Core, with special thanks to Juan Jimenez for his technical assistance.

Funding: This research and the open accessibility was funded by the National Institutes of Health – Pioneer Award, grant number 5DP1AT012812 to M.H. and an E.E. Just MBL Whitman Fellowship to M.H. The accessibility to the Transmission Electron Microscope at the Weill Cornell Medicine facility was granted by a NIH Shared Instrumentation Grant (S10RR027699) for Shared Resources. Manuscript contents are solely the responsibility of the authors and do not necessarily represent the official views of the NIH. The funders had

no role in study design, data collection and analysis, decision to publish or preparation of the manuscript.

Institutional Review Board Statement: The animal study protocol was approved by the Institutional Review Board (or Ethics Committee) of The Marine Biological Laboratory (protocol code 2023_MBL-IBC-36 approved June 16, 2023).

Author contributions: conceptualization, M.H. and K.N.K.; methodology, M.H., E.S., A.C., K.C., A.L.S., D.J.V., J.R.P.B., C.Ca., C.C. and M.W.; validation, M.H., E.S., A.C., K.C., A.L.S., D.J.V., J.R.P.B., C.Ca., C.C. and M.W.; formal analysis, K.N.K., M.H., E.S., A.C., K.C., A.L.S., D.J.V., J.R.P.B., C.Ca., C.C. and M.W.; investigation, K.N.K., M.H., E.S., A.C., K.C., A.L.S., D.J.V., J.R.P.B., C.Ca., C.C. and M.W.; resources, K.N.K. and M.H.; data curation, K.N.K, B.S., A.M., K.C., A.L.S., D.J.V., J.R.P.B., C.C. and M.W.; writing-original draft preparation, K.N.K, B.S., M.H. and M.W.; writing-review and editing, K.N.K., B.S., M.H., E.S., A.C., K.C., A.L.S., D.J.V., J.R.P.B., C.Ca., C.C. and M.W.; visualization, K.N.K., A.C., K.C., A.L.S., D.J.V., J.R.P.B., C.Ca., C.C. and B.S.; supervision, M.H.; project administration, M.H.; funding acquisition, M.H. All authors have read and agreed to the published version of the manuscript.

Competing interests: The authors declare no competing interests.

Data and materials availability: High-resolution digital scans of the *Octopus bimaculoides* hatchling and posterior salivary gland tissue sections are available at https://bio-atlas.psu.edu